⌘ *Author's Choice*

LytA, Major Autolysin of *Streptococcus pneumoniae*, Requires Access to Nascent Peptidoglycan*[S]

Peter Mellroth[‡1,2], **Robert Daniels**[§1], **Alice Eberhardt**[‡], **Daniel Rönnlund**[¶], **Hans Blom**[¶], **Jerker Widengren**[¶], **Staffan Normark**[‡], and **Birgitta Henriques-Normark**[‡||]

From the [‡]*Department of Microbiology, Tumor, and Cell Biology, Karolinska Institutet, 17177 Stockholm, Sweden, the* [§]*Center for Biomembrane Research, Department of Biochemistry and Biophysics, Stockholm University 10691 Stockholm, Sweden, the* [¶]*Experimental Biomolecular Physics, Department of Applied Physics, Royal Institute of Technology, Albanova University Center, 10691 Stockholm, Sweden, and the* [||]*Department of Laboratory Medicine, Division of Clinical Microbiology, Karolinska University Hospital, 17176 Stockholm, Sweden*

Background: The regulation of cell wall hydrolysis by the pneumococcal autolysin LytA is poorly understood.
Results: The cell wall is susceptible to extracellular LytA only during the stationary phase or after cell wall synthesis inhibition.
Conclusion: LytA is regulated on the substrate level, where peptidoglycan modifications likely prevent LytA hydrolysis.
Significance: The control of amidases is essential for bacterial survival, cell-wall synthesis, and division.

The pneumococcal autolysin LytA is a virulence factor involved in autolysis as well as in fratricidal- and penicillin-induced lysis. In this study, we used biochemical and molecular biological approaches to elucidate which factors control the cytoplasmic translocation and lytic activation of LytA. We show that LytA is mainly localized intracellularly, as only a small fraction was found attached to the extracellular cell wall. By manipulating the extracellular concentration of LytA, we found that the cells were protected from lysis during exponential growth, but not in the stationary phase, and that a defined threshold concentration of extracellular LytA dictates the onset of autolysis. Stalling growth through nutrient depletion, or the specific arrest of cell wall synthesis, sensitized cells for LytA-mediated lysis. Inhibition of cell wall association via the choline binding domain of an exogenously added enzymatically inactive form of LytA revealed a potential substrate for the amidase domain within the cell wall where the formation of nascent peptidoglycan occurs.

Streptococcus pneumoniae, or the pneumococcus, has a characteristic autolytic response that is induced during the stationary growth phase and leads to the excessive lysis of cultures *in vitro*. The induction of the pneumococcal autolytic response by the bile salt detergent deoxycholate was first discovered in 1900 and further characterized by Avery *et al.* (1–3) in the 1920s. Decades later autolysis was connected to penicillin-induced

lysis, (4, 5) the autolysin gene *lytA* was cloned, and the structure of its cell wall attachment domain was determined (6, 7).

LytA causes lysis by cleaving the lactyl-amide bond that links the stem peptides and the glycan strands of the peptidoglycan, resulting in hydrolysis of the cell wall (Fig. 1*A*) (8). LytA orthologs are now known to be conserved throughout eubacteria and in many bacteriophages (9, 10). Furthermore, related amidases are also present in eukaryotes, where they are termed peptidoglycan recognition proteins, and involved in innate immune responses (11–13).

Pneumococcal LytA is structurally organized as a two domain protein with an N-terminal *N*-acetylmuramoyl L-alanine amidase domain and a C-terminal choline binding domain (Fig. 1*B*). The choline binding domain enables the enzyme to bind to phosphocholine residues present on the teichoic acids of the cell wall (6). Cell wall attachment through the choline binding domain is required for LytA activity because choline concentrations that inhibit cell wall binding also prevent autolysis (14).

The *in vivo* function of LytA remains controversial. In murine infection models, LytA-deficient pneumococci are less virulent than parental wild-type strains, but how LytA contributes to pneumococcal virulence is not clear (15–17). One hypothesis is that LytA mediates lysis to release other virulence factors such as pneumolysin (18). Another theory suggests that LytA is released to lyse neighboring non-competent pneumococcal cells in a fratricidal manner (19). This would potentially facilitate genetic exchange between naturally competent pneumococcal populations that easily take up and incorporate DNA by homologous recombination. A third possibility is that LytA mediates lysis to release proteins involved in immune evasion or cell wall components that may interfere with the host immune response (20).

From a therapeutic perspective, LytA is known to contribute to the penicillin- and vancomycin-induced lysis of pneumococci (4, 5). Supporting the link between antibiotic treatment and LytA, penicillin and vancomycin resistance among clinical isolates has been shown to be partly related to the activity of

LytA (21, 22). Despite the numerous studies on LytA, several basic features of this protein still remain elusive. It is unclear what regulates its lytic activity, why lysis is triggered in a predictable timeframe following entry into the stationary phase, and how LytA is targeted to the cell wall.

In this study, we investigated the topological distribution of LytA during growth and the characteristics that contribute to its release and activity by creating chimeras with different signal sequences using choline inhibition, adding LytA exogenously, or treating the bacteria with detergent or different antibiotics. We confirm that pneumococci are protected from the lytic activity of LytA during exponential growth, but not in stationary phase (4), and propose a model on the basis of our data explaining why this occurs.

EXPERIMENTAL PROCEDURES

Cloning Procedures for Making Pneumococcal Mutant Strains and Vectors for Protein Expression in Escherichia coli—The cloning procedures are described in supplemental Methods and Figs. S1 and S2.

Pneumococcal Growth Conditions—Pneumococcal strains were grown either at 37 °C on blood agar (BA) plates incubated overnight with 5% CO_2 or in C+Y media (23) containing 1% horse serum in a water bath. To monitor growth kinetics and autolysis, pneumococci from a fresh BA plate were suspended in C+Y media to an $A_{600\,nm} = 0.1$, grown to $A_{600\,nm} = 0.5$, and again diluted to an $A_{600\,nm} = 0.05$ with C+Y media or with the indicated supplements. Cells were grown at 37 °C in a water bath or in multiwell plates within a Bioscreen instrument (Growthcurves OY) where the $A_{600\,nm}$ was recorded (24).

Pneumococcal Transformation—T4 cultures were inoculated in C+Y medium to an $A_{600\,nm} = 0.02$ and grown to $A_{600\,nm} = 0.1$ in a water bath at 37 °C. Cells were diluted 10-fold into tryptic soy broth with 10% glycerol and 0.01% $CaCl_2$ and incubated at 30 °C for 15 min. Competence stimulating peptide 2 was added. After 15 min, 0.5 μg of PCR product was administered, and the cells were incubated for an additional 60 min at 30 °C and then shifted to 37 °C for 90 min before spreading onto BA plates containing 2 mg/L of erythromycin. Resistant colonies were isolated, and the mutation was confirmed by sequencing the PCR-amplified *lytA* locus from the genomic DNA using primers that annealed ~100 bp upstream and downstream of the recombination site.

Blotting and Immunodetection—T4, T4/*lytA-erm*, and T4Δ*lytA* cultures were grown in C+Y media until $A_{600\,nm} = 0.5$. Samples of 200 μl were withdrawn, sedimented at 6000 × g for 2 min, resuspended in 1× SDS loading buffer, and boiled for 5 min. Proteins were separated on a 4–12% gradient gel (Invitrogen) and subsequently blotted onto a PVDF membrane and stained with Ponceau S (Sigma). Destaining was done with 0.1 M NaOH for 1 min, the membrane was probed with LytA antiserum (Agro-bio, France), and chemiluminescence detection was performed with ECL-plus (GE Healthcare).

Antibiotic and Deoxycholate Treatments—T4R strains were grown in C+Y with or without 1% choline chloride or recombinant LytA (1 μg/ml) in the Bioscreen. At $A_{600\,nm} = 0.28$, the bacteria were challenged with 1 μg/ml of penicillin G or vancomycin; 5 μg/ml of cefadroxil, rifampicin, or erythromycin; or 50 μg/ml of bacitracin or tetracyclin, and the $A_{600\,nm}$ was recorded. For deoxycholate activation of LytA, T4, and T4Δ*lytA*, cultures were grown in C+Y or C+Y supplemented with 1% choline chloride or recombinant LytA (1 μg/ml) in the Bioscreen, and at $A_{600\,nm} = 0.6$, deoxycholate was added to a final concentration of 0.6%.

Nutrient Depletion—Cultures of T4 and T4/*sp^{nanA}lytA-erm* were grown in Bioscreen wells in C+Y medium or in C+Y medium supplemented with recombinant LytA (5 μg/ml) or 1% choline chloride. At $A_{600\,nm} = 0.6$, the cultures were transferred to Eppendorf tubes, sedimented at 6000 × g for 2 min, and the supernatants were removed. The cultures were resuspended in 400 μl of PBS or C+Y or in PBS or C+Y supplemented with 1% choline. The cultures were then transferred back to Bioscreen wells, and the $A_{600\,nm}$ was followed.

In a second experiment, two 400-μl cultures of T4/*sp^{nanA}lytA-erm* were grown in the Bioscreen, and at $A_{600\,nm} \approx 0.5$, the cultures were sedimented and resuspended in 400 μl of PBS or C+Y. When the culture resuspended in PBS decreased to an $A_{600\,nm} = 0.1$, the cells were sedimented, and the supernatant was filtered through a 0.2-μm syringe filter (Pall). Four cultures of T4Δ*lytA* were grown to $A_{600\,nm} \approx 0.5$, after which the cultures were sedimented, resuspended in 300 μl of PBS or C+Y, and 100 μl of the filtered supernatant from the T4/*sp^{nanA}lytA-erm* culture or 100 μl of PBS was added and the cultures were transferred back to the Bioscreen.

LytA Topology Distribution Analysis—Samples (0.3 ml) from T4 cultures were taken at $A_{600\,nm} = 0.25, 0.5, 0.75, \sim 1.0$ (entry to stationary phase), ~1.0 (+2 h), ~1.0 (+4 h), ~1.0 (+6 h), and 0.9 (+7 h, 20 min after onset of autolysis). The samples from the culture grown in C+Y were sedimented at 6000 × g for 2 min, and the supernatant, representing the media fraction, was passed through a 0.2-μm filter and mixed with 100 μl 4× SDS loading buffer. To obtain the cell wall fraction, the pellet was resuspended in 300 μl of C+Y media supplemented with 1% choline chloride, incubated for 5 min, and sedimented at 6000 × g for 2 min. The filtered supernatant, representing the cell wall-attached fraction, was mixed with 100 μl of 4× SDS loading buffer. The pellet was resuspended and washed twice with C+Y with 1% choline chloride by centrifugation, and the pellet, representing the intracellular fraction, was lysed in 400 μl of 1× SDS loading buffer. The samples from cultures grown in C+Y with 1% choline chloride were treated similarly, except no cell wall-attached fraction was collected. To compensate for differences in bacterial concentration viable counts were determined for each of the respective time points, and the sample volumes were adjusted so that fractions equivalent to 7×10^7 viable bacteria were loaded onto the gel. Immunodetection was done as described, and the band intensities were quantified using the Image lab software (Bio-Rad).

Comparative topology distribution of LytA was done from growing T4, T4/*sp^{rrgB}lytA-erm,* and T4/*sp^{nanA}lytA-erm* cultures in C+Y or in C+Y + 1% choline chloride. Samples were taken at $A_{600\,nm} = 0.5$, sedimented at 6000 × g for 2 min, and then the supernatant was passed through a 0.2-μm syringe filter and mixed with SDS loading buffer, whereas the cells were washed with fresh C+Y and resuspended in SDS loading buffer. Samples were resolved on 4–12% polyacrylamide gel electro-

phoresis, blotted onto a PVDF membrane, and subjected to immunodetection using LytA antisera.

Recombinant Protein Production and Labeling—Recombinant LytA was produced in *E. coli* Rosetta 2 cells (Novagen) containing the pET21d-*lytA* or pET21d-*lytA[H26A]* expression vectors. Cells were grown in Luria broth (LB) (Sigma) at 37 °C with agitation and induced at $A_{600\,nm} = 0.5$ with 2 mM isopropyl 1-thio-β-D-galactopyranoside for 4 h. Cells were isolated by sedimentation and stored at -20 °C. The cell pellets were resuspended in lysis buffer (20 mM Tris (pH 7.5), 500 mM NaCl with lysozyme 2 mg/ml, DNase 200 μg/ml, and complete protease inhibitor mixture (Roche)) and rotated at 4 °C for 30 min. The cell suspension was lysed by four passages through a French press at 1500 psi, clarified by centrifugation, and passed over a DEAE fast flow Sepharose column (GE Healthcare). After washing with 20 column volumes of wash buffer (20 mM Tris (pH 7.5), 500 mM NaCl), the protein was eluted with wash buffer containing 140 mM choline chloride. Protein-containing fractions were pooled and dialyzed against 20 mM Tris (pH 7.5), 150 mM NaCl, 5 mM choline chloride, and 1 μM ZnCl$_2$. Protein concentration was determined by reading the absorbance at 280 nm using the molar extinction coefficient 115,530 cm/M and the molecular mass 36.5 kDa. LytA was labeled with the Alexa Fluor 594 protein labeling kit (Invitrogen) according to the manufacturer's directions.

Staining of Pneumococcal Cells—For live-cell imaging, cultures of T4Δ*lytA* were grown, and at $A_{600\,nm} = 0.3$, recombinant LytA labeled with Alexa Fluor 594 was added from a 1-mg/ml stock solution to a final concentration of 10 μg/ml. Unlabeled LytA and buffer (PBS) were given to control cultures. At $A_{600\,nm} = 0.5$, a sample was taken from the LytA-Alexa Fluor 594-challenged culture, and the cells were washed twice with C+Y medium through sedimentation at 6000 $\times$ *g* for 2 min, concentrated 10-fold, and applied to a microscopy slide coated with an approximately 1-μm-thin agarose pad.

For high-resolution imaging, T4Δ*lytA* cells were grown in C+Y to $A_{600\,nm} = 0.5$, sedimented at 6000 $\times$ *g* for 2 min, and fixed with 2% paraformaldehyde and 0.05% glutaraldehyde in PBS for 20 min. High-precision coverslips (no. 1.5, Marienfeld) were precoated with 10% BSA in PBS for 10 min, and the cells were spread and dried on the coverslip and then heat-fixed for 5 s at 150 °C. Samples were rehydrated with PBS and incubated with Alexa Fluor 594-labeled LytA or LytA-H26A (10 μg/ml) in PBS + 1% BSA for 5 min at 20 °C. The coverslips were extensively washed with PBS to remove unbound protein and mounted using ProLong Gold antifade reagent (Invitrogen).

To study amidase-mediated cell wall interaction, T4Δ*lytA* cells were grown in C+Y to $A_{600\,nm} = 0.5$, after which cells were sedimented and resuspended in C+Y or C+Y with 1% choline. Alexa Fluor 594-labeled recombinant LytA-H26A was added to a final concentration of 10 μg/ml and incubated for 10 min. The cells were washed three times with C+Y with 1% choline, after which the cells were fixed and mounted on coverslips. To determine the relative amount of LytA associated with the cells following the treatment, a dot blot analysis was performed in parallel where the cells were diluted in 5-fold series, spotted onto a nitrocellulose membrane, and detected using LytA antisera.

Microscopy—For live-cell imaging, the prepared cells were immediately imaged using a Leica (DMRE) epi-fluorescence imaging system. The same system was also used for epi-fluorescence imaging of fixed cells. Confocal and STED[3] images were acquired using a custom-built microscope described previously (25, 26) equipped with a supercontinuum laser (SC-450-PP-HE, Fianium Ltd., Southampton, UK) with an applied repetition rate of 1 MHz and pulse width of ~100 ps. The excitation and STED beams are coupled together using a dichroic mirror (z690SPRDC, Chroma Technology Corp.) before being sent into the microscope objective. Images were obtained using a scanning piezo stage attached to a closed loop controller (MAX311/M and BPC203, Thorlabs, Sweden AB) that offers a positional resolution of 5 nm. The fluorescence from the labeled sample is collected back through the objective and separated from the excitation and the STED beams by a customized dichroic mirror (Laseroptik, Garbsen, Germany). The image size was set to 5 $\times$ 5 or 7 $\times$ 7 μm^2 with a pixel size of 20 nm for the STED images and 50 nm for the confocal images. The pixel dwell time was 1 ms with 500–1000 nW excitation laser power and 2.2 milliwatt STED laser power.

RESULTS AND DISCUSSION

Genetic Strategy to Address LytA Function and Localization—The pneumococcal autolysin LytA is one of the most intensely studied cell wall degrading amidases. Still, several fundamental features of this suicide enzyme remain elusive. We have combined genetic and biochemical approaches to investigate and manipulate the topological distribution of LytA and to examine which factors regulate its hydrolytic activity. To investigate the requirements of LytA activation, we established a genetic system that enabled the insertion of various LytA mutants into the LytA locus. Initially, we cloned the *lytA* coding sequence with the 1000 bp up- and downstream of the coding sequence from *S. pneumoniae* T4 into a cloning vector. We then replaced the *lytA* coding sequence with an erythromycin cassette to create a plasmid Δ*lytA*. To account for any polar effects introduced by the *erm* insertion, we also inserted the *erm* cassette immediately after the stop codon of *lytA* to create the plasmid *lytA-erm* (Fig. 1*B*). PCR amplicons of Δ*lytA* and *lytA-erm*, which covered the 1-kb *lytA* flanking regions, were used to transform T4 to create T4Δ*lytA*, a strain devoid of LytA, and the control strain T4/*lytA-erm*.

The feasibility of this approach was examined by comparing the growth and autolysis profiles of T4Δ*lytA* and T4/*lytA-erm* to that of the wild-type T4 strain (Fig. 1*C*). The growth curve of T4 was typical for *S. pneumoniae* and T4Δ*lytA* showed the characteristic loss of autolysis (27). The T4/*lytA-erm* strain showed a similar growth profile as T4, with the exception that autolysis was triggered at a slightly later time point. LytA immunoblots of whole cell lysates confirmed that LytA is not produced in T4Δ*lytA* and that T4/*lytA-erm* produces LytA at a slightly lower level than T4 (Fig. 1*D*). This suggests that the decreased production of LytA in T4/*lytA-erm* is responsible for the delayed autolysis profile, implying that there is a correlation

---

[3] The abbreviations used are: STED, stimulated emission depletion microscopy; sp, signal peptide; recLytA, recombinant LytA.
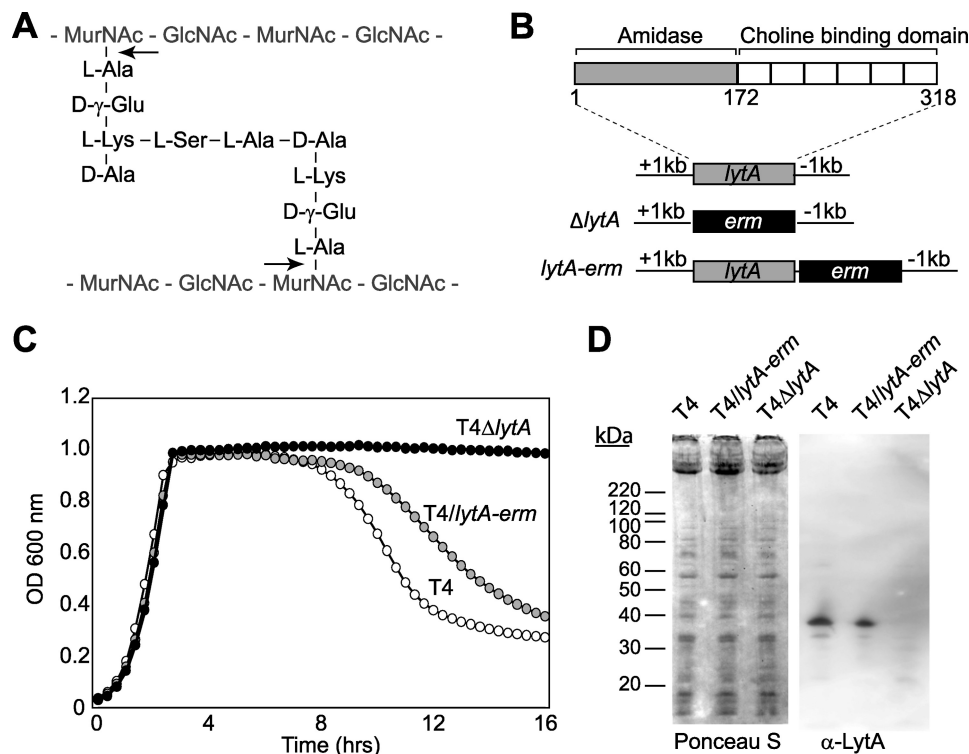
FIGURE 1. **LytA function and genetic strategy.** *A*, LytA is an *N*-acetylmuramoyl L-alanine amidase that cleaves the peptidoglycan by hydrolyzing the lactyl-amide bond (*arrows*) that links the peptides and the glycan strands. *MurNAc*, *N*-acetyl muramic acid; *GlcNAc*, *N*-acetyl glucosamine. *B*, schematic depicting the LytA amidase and choline binding domains and the genetic organization of the Δ*lytA* and *lytA-erm* mutants with respect to the *lytA* locus. *C*, growth profiles demonstrating that the TIGR4 (T4) *S. pneumoniae* mutant T4Δ*lytA* has a non-autolytic phenotype and that the T4/*lytA-erm* strain has a slight delay in autolysis compared with T4. *D*, Ponceau S staining and immunoblot detection of lysates from mid-log cultures ($A_{600 \, nm}$ = 0.5) of the indicated T4 strains using LytA antisera.

between the amount of LytA that is synthesized and the onset of autolysis. The reduction of LytA synthesis in T4/*lytA-erm* also indicated that elements downstream of *lytA* weakly influence its expression.

LytA Resides Mainly in the Cytoplasm—Choline binding proteins are cell wall-associated proteins that bind to choline residues within the teichoic acids of the *S. pneumoniae* cell wall (28). Thus, most choline binding proteins contain an N-terminal signal peptide that targets them to the extracellular cell wall via translocation across the plasma membrane through the SecYEG translocon (29). However, LytA does not contain any discernible motif for protein secretion. This would predict LytA to localize within the cytoplasm, but to reach the cell wall and cleave peptidoglycan, LytA must somehow translocate from the cytoplasm. To determine the topological distribution of LytA, we investigated samples taken from a pneumococcal culture during the logarithmic and stationary phase and soon after the onset of autolysis (*i.e.* Fig. 2*A*, time points *a–h*). By analyzing the ratio of intracellular *versus* extracellular LytA located in the cell wall or in the media, we found that the majority of LytA (~95%) resides in the cytoplasm during logarithmic growth, whereas only a small fraction (~5%) was associated with the extracellular cell wall (Fig. 2*B*, samples *a–c*). During the stationary phase, the extracellular fraction of LytA slowly increases to ~30%, after which autolysis is induced, and a major release of LytA results from cellular lysis (Fig. 2*B*, samples *d–h*).

Because only a minor fraction of LytA was found extracellularly, we considered the possibility that the cytoplasmic "trans-

location" could be due to cellular lysis and not active secretion. It is likely that some cell turnover occurs during logarithmic growth, resulting in the release of LytA and its rebinding to neighboring cells. Also fratricidal lysis in the early logarithmic phase, which is a DNA competence-dependent response mediated by CbpD, LytC, and LytA, could contribute (19, 30, 31). To investigate if lysis mediated by choline binding hydrolases accounted for the ~5% of LytA that localized extracellularly during logarithmic growth, we analyzed the topology distribution of LytA in T4 cells grown in the presence of 1% choline, which inhibits autolysis as well as the association of other choline binding proteins with the cell wall (Fig. 2*A*). Indeed, a smaller fraction (~1%) of the total LytA population was present extracellularly, and no prominent accumulation occurred during the stationary phase (Fig. 2*C*). Thus, our data indicate that the cytoplasmic release of LytA during logarithmic growth and its extracellular accumulation in the stationary phase is mainly due to fratricidal lysis or cell turnover mediated by choline binding hydrolases and not by active secretion.

Active Secretion of LytA Initiates Autolysis upon Entry into the Stationary Phase—Because the majority of LytA resides in the cytoplasm, we wanted to investigate what happens if LytA is shifted to a predominantly extracellular topology distribution. To accomplish this, we created T4 strains that encoded for LytA fused to two different N-terminal signal peptides (sp) (Fig. 3*A* and supplemental Figs. S1 and S2). One strain, T4/*sp^{rrgB}lytA-erm*, used a classical sp taken from the pneumococcal pilus subunit RrgB that should direct the secretion of
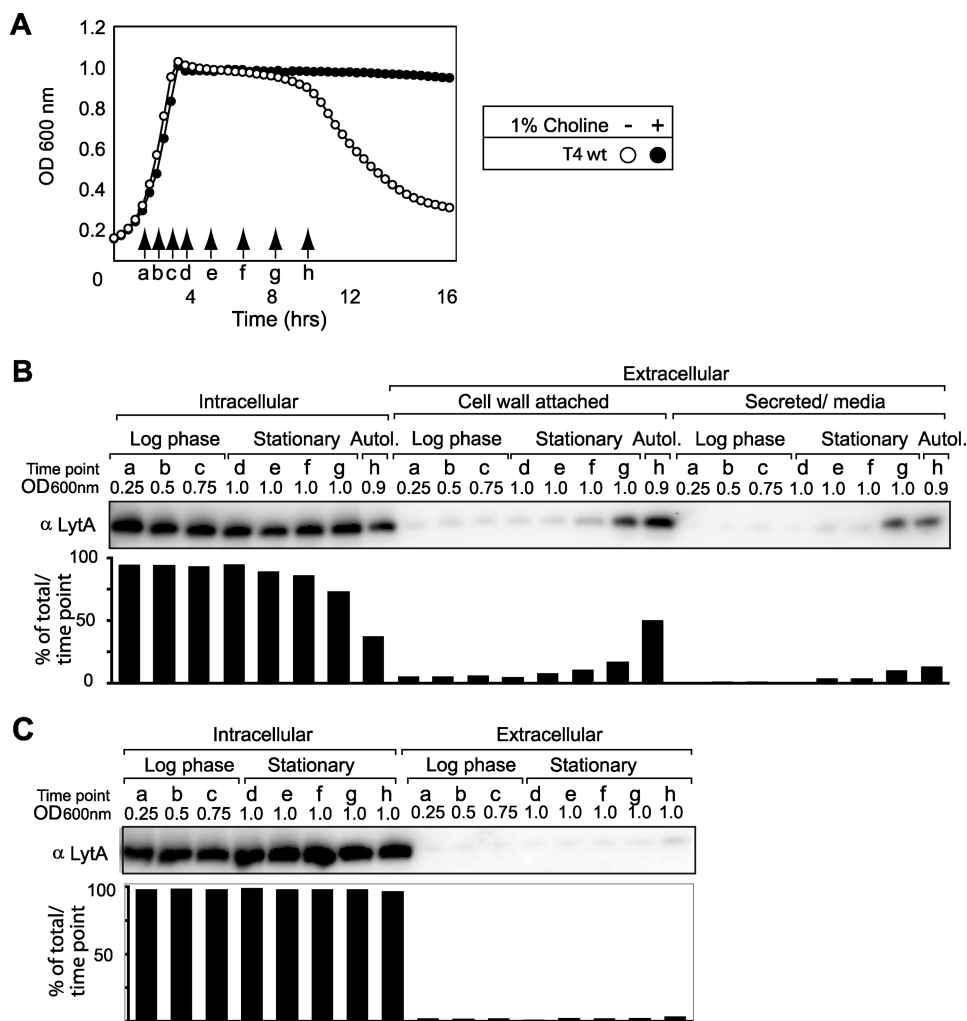
FIGURE 2. **LytA topology distribution in *S. pneumoniae*.** *A*, growth profile of T4 grown in C+Y media with or without 1% choline chloride. Samples *a–h* were withdrawn at the indicated time points to investigate the protein topology. *B*, topology distribution of LytA assayed by immunoblot analysis. Samples *a–h* (depicted in *A*) were taken from growing cultures at different OD:s in the log-phase and after 0 h (*d*), 1.5 h (*e*), 3 h (*f*), 4.5 h (*g*) in stationary phase and at 30 min (*h*) after autolysis was initiated. The percentage of the total LytA detected intracellularly, cell wall-attached, or secreted into the media was analyzed for each time point. *C*, topology distribution of LytA from T4 grown in C+Y media with 1% choline assayed by immunoblot analysis. The amount of LytA detected in the intracellular fractions *versus* extracellular fractions (all present in the media fraction because cell wall attachment was prevented by 1% choline) was analyzed for each time point (*a–h*).

LytA around the cell, whereas the second strain, T4/*sp^{nanA}lytA-erm*, used the YSIRK-motif containing pneumococcal NanA sp, which is thought to target secreted proteins to the cell division plane (32, 33).

In comparison to T4, the growth profiles of T4/*sp^{rrgB}lytA-erm* and T4/*sp^{nanA}lytA-erm* in C+Y media were similar during the logarithmic phase. However, both strains displayed a prominent phenotype as their autolysis was induced soon after entry into the stationary phase. The kinetics of autolysis was more rapid in the T4/*sp^{nanA}lytA-erm* strain (Fig. 3*B*). These results show that a high extracellular LytA concentration does not impact growth in the logarithmic phase, but it does influence the timing and rate of autolysis in stationary phase. To determine the secretion efficiency for the two LytA constructs and whether they bound to the cell wall during the logarithmic phase, the ratio of intracellular to extracellular secreted and cell wall-attached LytA was examined from cultures in mid-log phase with an $A_{600\,nm} = 0.5$. During logarithmic growth in C+Y growth medium, the secreted versions of LytA were found both cell-associated (~50%) and in the media (Fig. 3*C, upper panel, lanes 3–6*). With 1% choline included in the growth media to prevent cell wall attachment, almost all of the LytA in T4/*sp^{rrgB}lytA-erm* and T4/*sp^{nanA}lytA-erm* was found in the media fraction, confirming that LytA was efficiently secreted in both strains (Fig. 3*C, bottom panel, lanes 3–6*). These results imply that the cells are protected from the cell wall hydrolytic activity of LytA during logarithmic growth and that the protective features are lost upon entry to the stationary phase.

Extracellular LytA Concentrations Dictate When Autolysis Occurs in the Stationary Phase—To better manipulate the extracellular concentration of LytA, we produced and purified recombinant LytA (recLytA) from *E. coli* extracts (Fig. 3*D*). We then grew T4 and T4Δ*lytA* cultures in the presence of increasing amounts of recLytA (Fig. 3, *E* and *F*). The presence of recLytA in the culture medium did not alter the logarithmic growth kinetics of either strain, confirming that pneumococcal cells are protected from LytA-mediated lysis during logarithmic growth (4). However, this protective fea-
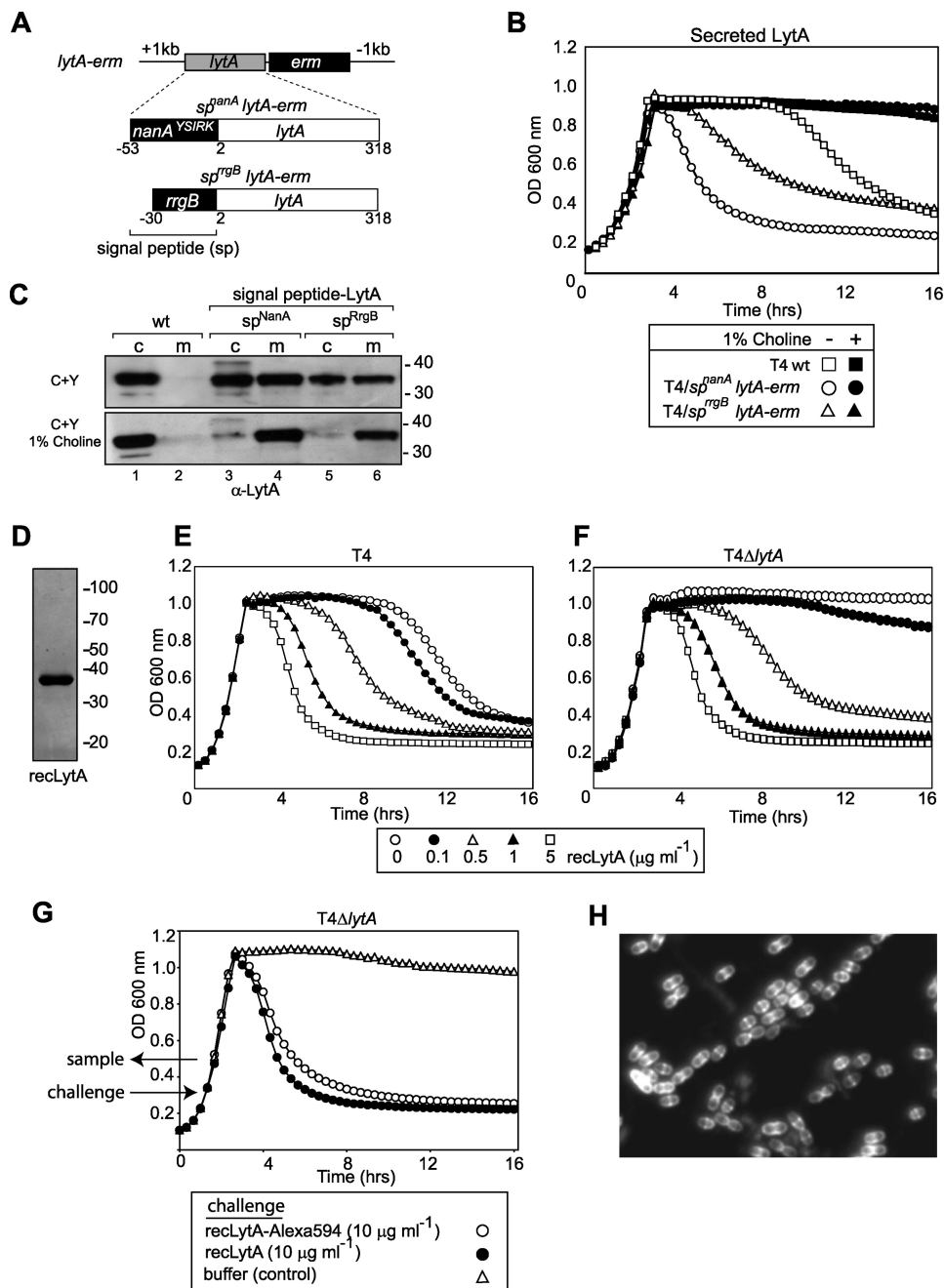
FIGURE 3. **Extracellular concentration of LytA dictates autolysis onset during stationary phase.** *A*, schematic of the T4 genomic replacements encoding for secreted LytA with a signal peptide from *nanA* or *rrgB* expressed from the *lytA* cognate promoter. *B*, growth kinetics of the T4 strains secreting LytA in the presence or absence of 1% choline. *C*, immunoblot analysis of LytA localization in the different strains at an $A_{600\,nm} = 0.5$. Cell-associated LytA (*c*) was compared with LytA secreted into the media (*m*) in the absence and presence of 1% choline. *D*, Coomassie-stained gel of recombinant LytA purified from *E. coli*. *E* and *F*, growth curves displaying how culturing T4 and T4Δ*lytA* with the indicated amounts of recLytA had a dose-dependent effect on lysis in the stationary phase. *G*, growth curve of T4Δ*lytA* cultures challenged with Alexa Fluor 594-labeled recLytA, unlabeled recLytA (10 μg/ml), or buffer at $A_{600\,nm} = 0.3$. A sample was withdrawn at $A_{600\,nm} = 0.5$ after challenge with recLytA-Alexa Fluor 594 for epi-fluorescence live-cell imaging (*H*).

ture is lost after the transition to the stationary phase, as the recLytA had a dose-dependent influence on the timing of autolysis induction. When 5 μg/ml of recLytA was present, autolysis was induced immediately after entry into the stationary phase in both T4 and T4Δ*lytA* cultures (Fig. 3, *E* and *F*). Autolysis in response to 0.5 μg/ml of recLytA initiated soon after entry into stationary phase and showed a similar lytic kinetic phenotype in both T4 and T4Δ*lytA*. This suggests that 0.5 μg/ml is close to the threshold concentration

that is required to induce autolysis. At lower concentrations of recLytA (0.1 μg/ml), a contribution of cytosolic LytA was required to reach the threshold explaining the delay in autolysis onset in T4 and the loss of the normal autolytic response in the T4Δ*lytA* strain (Fig. 3, *E* and *F*). These results combined with those from the strains T4/*sp^{rrgB}lytA-erm* and T4/*sp^{nanA}lytA-erm*, which secretes LytA, implies that pneumococci are protected from LytA during logarithmic growth but not in stationary phase and that the initiation of autolysis

is dictated by the extracellular concentration of LytA with a threshold concentration near 0.5 μg/ml or 14 nM.

LytA Binds to the Cell Wall during Logarithmic Growth without Inducing Lysis—To address whether LytA interacts with the cell wall during logarithmic growth without causing lysis or growth inhibition, we challenged a growing culture of T4$\Delta lytA$ with an Alexa Fluor 594-labeled recombinant LytA at $A_{600\,nm}$ = 0.3, which had similar lytic activity as the unlabeled recombinant LytA (Fig. 3G). When the culture reached $A_{600\,nm}$ = 0.5, a sample was withdrawn for live-cell imaging using epi-fluorescence microscopy. Indeed, LytA bound throughout the cell wall and showed an intense staining in the equatorial region and at the division sites (Fig. 3H). Thus, LytA may sit abundantly cell wall-associated during logarithmic growth without causing lysis.

Deoxycholate Activates LytA in the Logarithmic Phase—The bile salt detergent deoxycholate is well known for its property to induce a prominent autolytic response in pneumococci (1, 2). Therefore, we decided to analyze whether deoxycholate could abrogate the LytA-protective features and induce LytA-mediated lysis in the logarithmic phase. We exposed T4 and T4$\Delta lytA$ cultures to 0.6% deoxycholate at $A_{600\,nm}$ = 0.6 and recorded changes in the absorbance to determine when LytA was activated to induce autolysis. Our data show that deoxycholate treatment induced the rapid lysis of T4 but not of T4$\Delta lytA$ (Fig. 4A). The LytA dependence was demonstrated by the addition of recLytA, which restored the rapid deoxycholate-triggered autolysis in T4$\Delta lytA$ and by the inhibition of deoxycholate-triggered autolysis when 1% choline was present. Analyzing the viability of the cells after deoxycholate treatment revealed that the treatment also efficiently killed the cells, as no viable colonies were obtained 5 min after the deoxycholate treatment of the T4$\Delta lytA$, which did not show a lytic phenotype. Because deoxycholate has detergent properties, the loss of viability is likely due to interference with the plasma membrane. To investigate if deoxycholate challenge caused membrane perturbation and release of LytA from the cytoplasm, we determined the amount of extracellular LytA in a culture in presence of 1% choline after treatment with deoxycholate (Fig. 4B). Indeed, deoxycholate was found to cause a substantial release of intracellular LytA within 3 min of addition. The synchronized halting of growth and release of intracellular LytA explains why the kinetic of lysis is so rapid after deoxycholate treatment. These findings suggest that pneumococcal viability is crucial to maintain a LytA protective phenotype, indicating that a membrane-associated function could be involved in the control of LytA activation.

Growth Inhibition Can Activate LytA-induced Lysis—Our data so far indicated that LytA is normally inactive during logarithmic growth but not in the stationary phase. We reasoned that this could either be due to a timely conversion of the enzyme to an active state after entry into the stationary phase or else that the peptidoglycan substrate is somehow made accessible when growth is halted. Deoxycholate treatment induced activation of LytA in the logarithmic phase, which indicated that a growth mechanism-related function could be involved in the regulation of LytA. To address these questions, we investigated the effect of halting growth through nutrient depletion in

the logarithmic phase by replacing the C+Y culture medium with PBS. T4 and T4/$sp^{nanA}lytA$-erm cultures were grown in C+Y media with or without recombinant LytA or 1% choline. At $A_{600\,nm}$ ≈ 0.6, the cultures were sedimented and resuspended in either PBS or C+Y with or without 1% choline (Fig. 4C). As expected, nutrient removal by replacing the media with PBS caused an immediate stalling of growth of the T4 strain, as the $A_{600\,nm}$ remained stable for several hours. Resuspension of the cells in PBS containing recLytA resulted in the rapid initiation of lysis but not when the resuspension was performed with C+Y, where the cells continued to grow and were only lysed after they entered the stationary phase. For the T4/$sp^{nanA}lytA$-erm strain, which secretes LytA, the PBS-stalled growth caused lysis to be induced in the absence of recLytA, and this lysis could be inhibited by 1% choline (Fig. 4D).

To further analyze whether LytA activity is controlled at the enzyme level and possibly converted form an inactive zymogen to an active form, we performed the following experiment. Lysis was induced in a T4/$sp^{nanA}lytA$-erm culture by nutrient depletion, and when the $A_{600\,nm}$ had dropped to ≈ 0.1, the supernatant was collected by centrifugation and filtered to ensure that no cells were present. The filtered supernatant from this lysed culture was supplied to mid-log cultures of T4$\Delta lytA$ that were sedimented and resuspended either in PBS or C+Y. The LytA-containing supernatant induced the immediate lysis of the T4$\Delta lytA$ cells resuspended in PBS but not C+Y (Fig. 4E). Thus, the activity of LytA is not controlled at the enzymatic level because an already "activated" LytA could not induce lysis to a growing T4$\Delta lytA$. Instead, these data strongly suggest that stalling of growth by nutrient removal sensitizes the cells to LytA-mediated lysis and that LytA is controlled at the substrate level in a process that is regulated by growth.

Inhibition of the Peptidoglycan Synthesis Machinery Activates LytA—To dissect what type of growth inhibition sensitizes pneumococci to LytA-dependent lysis, we employed various antibiotics that interfere with different cellular processes and assayed their ability to induce autolysis. To accentuate the potential LytA-dependent lytic response, we added an extra on-switch to the C+Y media in the form of recLytA (1 μg/ml) or an off-switch by including 1% choline. We then challenged T4R, an unencapsulated derivate of T4 that responds faster to antibiotics, with penicillin, cefadroxil, vancomycin, and bacitracin, which target the cell wall synthesis machinery and its lipid II substrate; erythromycin and tetracycline, which inhibit protein synthesis; rifampicin, which interferes with RNA transcription; and optochin, which affects a proton pump in the plasma membrane (Fig. 5A).

Of this panel of inhibitors, T4R became susceptible to LytA only in the presence of antibiotics that inhibit growth by blocking cell wall synthesis. With penicillin, cefadroxil, vancomycin, and bacitracin, the LytA dependence was verified by the potentiated lytic effect observed when recLytA was present and by the growth inhibitory, but non-lytic, response when 1% choline was present (Fig. 5A). As a control, the T4R$\Delta lytA$ strain showed a non-lytic phenotype toward cell wall targeting antibiotics, but in the presence of recLytA, the lytic phenotype was restored (supplemental Fig. S3). In contrast, T4R treated with antibiotics with other targets than the cell wall synthesis machinery caused
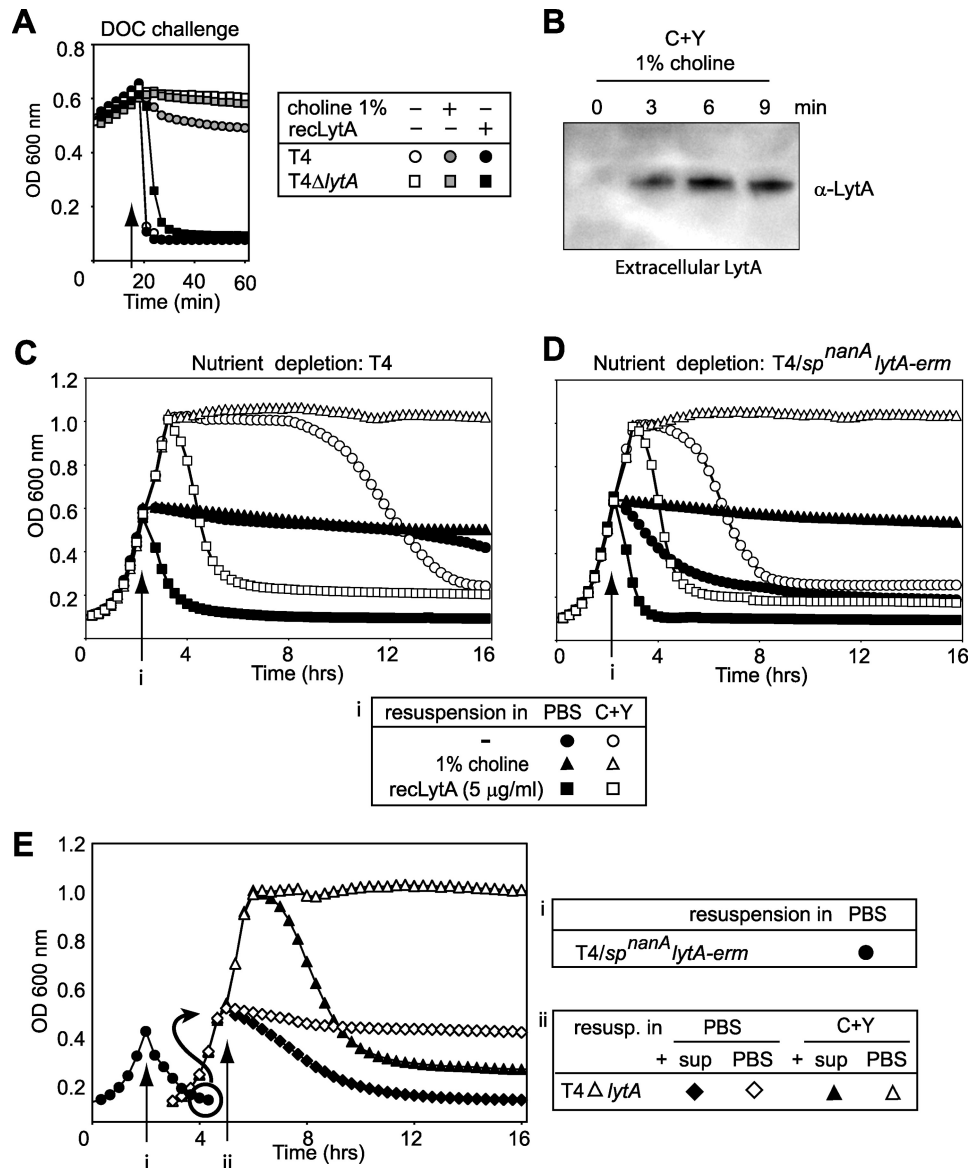
FIGURE 4. **Disrupting growth during the logarithmic phase may induce sensitivity towards LytA.** *A*, deoxycholate (*DOC*) challenge during logarithmic growth activates LytA-mediated lysis. Deoxycholate (0.6%) was added at $A_{600\,nm} = 0.6$ to T4 and T4Δ*lytA* cultures grown in C+Y media in the absence or presence of 1% choline or recLytA (1 μg/ml), and lysis was monitored by a decrease in optical density. B, Deoxycholate perturbs the membrane facilitating the release of intracellular LytA. Shown is an immunoblot analysis displaying the LytA released into the media from T4 cells grown in the presence of 1% choline and sampled at the indicated times after the addition of 0.6% deoxycholate. *C* and *D*, nutrient depletion sensitizes pneumococci to LytA-mediated lysis. Cultures of T4 (*C*) and T4/*sp^{nanA}lytA-erm* (*D*) were grown in C+Y media (● and ○) or C+Y supplemented with 1% choline (▲ and △) or recLytA (5 μg/ml) (■ and □). At $A_{600\,nm} \approx 0.6$ (*arrows*), bacteria was sedimented and resuspended in PBS (●, ▲, and ■) or C+Y (○, △, and □) with or without 1% choline or recLytA. *E*, LytA activation does not happen at the enzymatic level. T4/*sp^{nanA}lytA-erm* (●) was grown to $A_{600\,nm}$ nm ≈ 0.5 (*arrow*), centrifuged, and resuspended in PBS. When the culture reached $A_{600\,nm} \approx 0.1$, it was centrifuged, and the filtered supernatant was included in the resuspension mixture of T4Δ*lytA* cultures that were sedimented at $A_{600\,nm} \approx 0.5$ and resuspended in 300 μl of PBS or C+Y (plus the 100 μl from the lysed T4/*sp^{nanA}lytA-erm* supernatant).

the stalling of growth, but did not confer a LytA-susceptible phenotype (Fig. 5*A*).

These data strongly indicate that the cell wall synthesis machinery prevents LytA activation and that the requirement of growth inhibition for LytA activation is derived from the link between cell wall synthesis and growth. The observation that lysis was not observed following *e.g.* rifampicin treatment in the presence of excessive amounts of recLytA excludes the possibility that LytA is continuously processing the cell wall and that growth or lysis is a consequence of a balanced competition between cell wall synthesis and degradation.

Next, we considered the possibility that the bacteriolytic activity of the cell wall targeting antibiotic function by causing membrane perturbation and the release of intracellular LytA. To address this, we grew T4R in C+Y in the presence or absence of 1% choline, challenged the cultures with penicillin at $A_{600\,nm} = 0.28$, and monitored the release of LytA by immunoblotting. When grown in C+Y, we recorded increasing levels of extracellular LytA from 5 min to 20 min after penicillin treatment, but no such increase was observed when 1% choline was present (Fig. 5*B*). These findings show that penicillin does not cause LytA release through membrane perturbation. Instead,
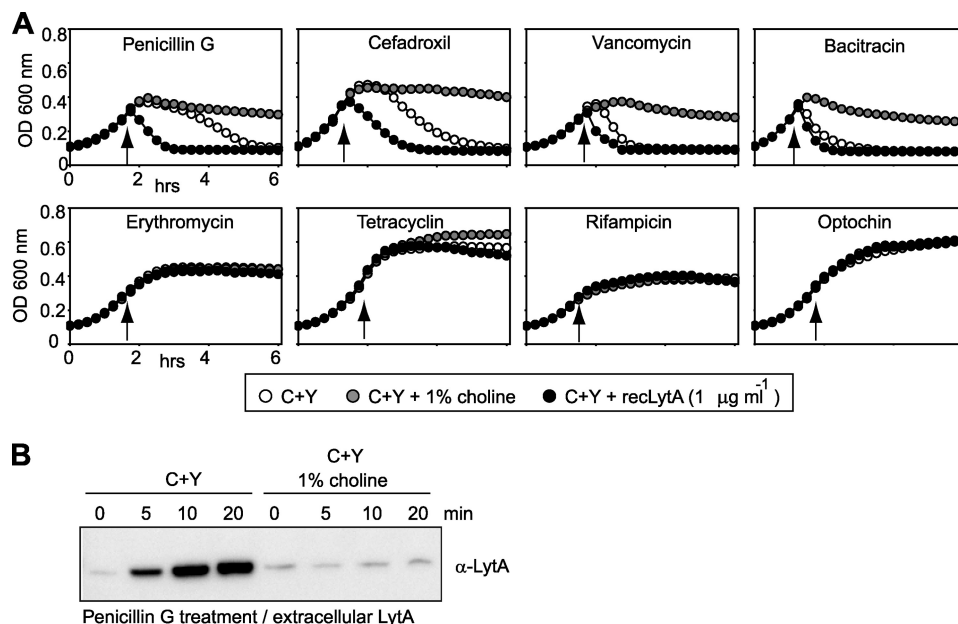
FIGURE 5. **Cell wall synthesis inhibition during logarithmic growth enables LytA to lyse pneumococci.** *A*, growth profiles of T4R cultures grown in C+Y in the absence or presence of recLytA (1 μg/ml) or 1% choline and challenged with the indicated antibiotics at $A_{600\ nm} = 0.28$ (*arrow*). *B*, penicillin does not perturb the bacterial membrane. Shown is the immunoblot analysis of the extracellular amount of LytA following the penicillin G treatment of T4R cultures grown in the absence or presence of 1% choline.

penicillin treatment renders T4R susceptible to the small amount of LytA that preexists in the cell wall, and this small amount facilitates the release of the cytoplasmic LytA via a lytic cascade. These data are in consonance with previous studies that have shown that β-lactam antibiotics and vancomycin mediate a LytA-dependent lysis, and our results additionally demonstrate that bacitracin activates LytA (4, 5). Together, these data strongly suggests that the key mechanism to the control of the lytic activity of LytA is directly related to the process of cell wall growth.

LytA Interacts with Peptidoglycan at the Equatorial Division Site—To understand how LytA could be regulated through factors related to the cell wall synthesis machinery, we sought to visualize where LytA localizes on the cell wall. To examine the cell wall interaction of LytA via its amidase domain, we produced an enzymatically inactive form of LytA by mutating a histidine residue (His-26) that was recognized as a putative zinc ligand on the basis of the homology to His-60 of the *Staphylococcus epidermidis* autolysin AmiE (34). Recombinant LytA[H26A] was produced and was found to be enzymatically inactive, as it did not cause lysis when it was added to a stationary phase T4Δ*lytA* culture (supplemental Fig. S4).

Fluorescently labeled LytA and LytA[H26A] were then incubated with fixed T4 cells from mid-log phase, and the cells were visualized with different microscopic techniques. Both LytA and LytA[H26A] displayed binding throughout the cell wall but more intensely in zones at the mid-cell region and at septal division sites (Fig. 6, *A* and *B*, confocal and epi-fluorescence). This staining pattern was observed in the vast majority of cells, 87% of LytA-stained cells and 83% of LytA[H26A]-stained cells, as determined from large-field epi-fluorescence images. To better resolve the localization, we used high-resolution STED microscopy. With STED

microscopy, both forms of LytA appeared to localize to the entire cell wall as well as to a more prominent band localized at the equatorial plane and at the site of the septum of dividing cells.

Because the enzymatically inactive LytA[H26A] may remain bound after substrate recognition, we attempted to use this property to identify potential binding sites of the amidase domain on the cell wall. First, we incubated T4 cells with LytA[H26A] in C+Y containing 1% choline to prevent cell wall binding via the choline binding domain of LytA. Under these conditions, we could not detect any cell wall staining (data not shown). However, we reasoned that the initial attachment to the cell wall through the choline binding domain might be instrumental for the correct positioning of the amidase domain relative to its substrate. Thus, we administered excessive amounts of LytA[H26A] to exponentially growing T4 cells at $A_{600\ nm} \approx 0.5$. The cells were then washed and incubated with C+Y containing 1% choline for three consecutive 5-min periods. This was done to release and inhibit cell wall interactions of LytA through its choline binding domain and leave only the LytA that was bound via its amidase domain. Interestingly, this treatment induced a staining pattern consisting of two bands located adjacent to the equatorial plane and observed in 85% of the cells (Fig. 6C). In comparison to the choline-dependent staining (Fig. 6B), most of the protein that evenly stained the cell wall was removed. Also, the equatorial band was gone and had been replaced with two new bands that were in close proximity to the equator. These bands stained weaker in intensity and required longer exposure time than the choline-dependent staining (Fig. 6B) but was consistent after several washings with 1% choline. The staining pattern was best resolved using STED microscopy (Fig. 6C), which has a resolution close to 40 nm, revealing an empty equatorial cleft flanked by two proximal bands. The interaction of LytA with
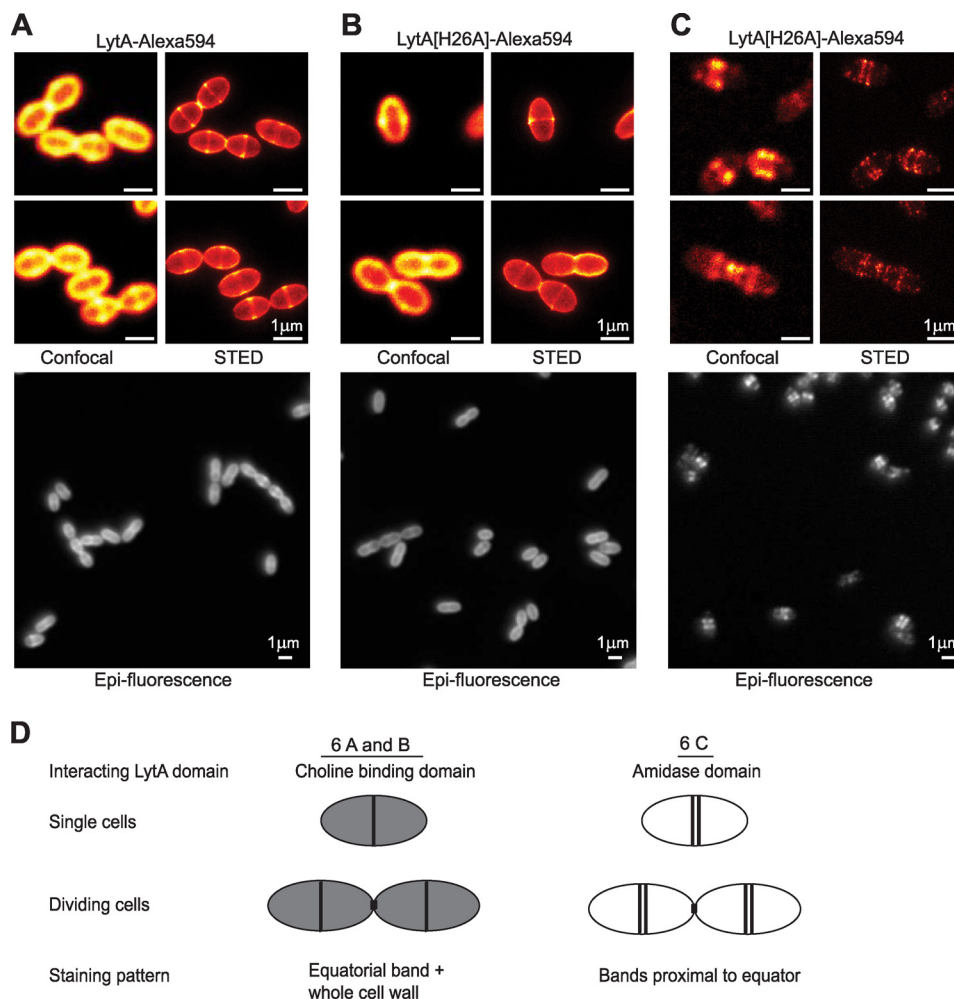
FIGURE 6. **A substrate for LytA adjacent to the equatorial plane.** *A* and *B*, confocal, STED, and epi-fluorescence images of T4Δ*lytA* cells from the logarithmic phase stained with Alexa Fluor 594-labeled LytA and LytA[H26A]. *C*, amidase-bound LytA. Mid-logarithmic phase T4Δ*lytA* cells were incubated with LytA[H26A]-Alexa Fluor 549 and then consecutively washed and incubated with 1% choline in C+Y to dissociate the choline-bound LytA. *D*, summary of *A–C* treatments and LytA staining patterns.

cells was further examined by a dot blot analysis. These results confirms that only a minor fraction of LytA takes part in the choline-independent interaction and that no interaction is observed if LytA is distributed with 1% choline present from the start (supplemental Fig. S5).

The cell wall of pneumococcus grows at the equatorial mid-cell and is synthesized by penicillin-binding proteins that incorporate new muropeptide building blocks through transglycosylation and transpeptidation (35). Further modifications and maturation of the cell wall are thought to occur after its incorporation (36, 37). Thus, the binding pattern of the inactive form of LytA colocalizes with the nascent premature peptidoglycan that likely represents the substrate that the amidase domain initially acts on (Fig. 6D).

The presence of a substrate for the amidase domain of LytA that colocalizes with the nascent peptidoglycan opens up the possibility that LytA requires a specific substrate to initiate lysis. The fact that LytA may occupy the cell wall during logarithmic growth without inducing lysis indicates that the intact cell wall is inaccessible as a substrate for LytA. We therefore suggest that the mature peptidoglycan is capped to confer protection from the lytic activities of LytA.

The capping could possibly be formed during the final steps of the peptidoglycan synthesis process in which the nascent peptidoglycan matures, and it could consist of some type of modification.

Peptidoglycan is frequently modified, and some of these modifications affect the activity of cell wall lytic enzymes. Modifications of the glycan strands are reported to occur after cell wall incorporation, and *N*-deacetylation and *O*-acetylation are examples of modifications that have been reported to confer an inhibitory effect on the activity of cell wall hydrolytic enzymes (36, 37). Also, the degree or mode of peptide cross-linking could potentially serve as a cap, and this has been reported to confer a resistance phenotype toward penicillin (38). However, it is likely that a mutant lacking the LytA protective cap has not yet been identified because it would probably be lethal in a wild-type background.

In contrast, the region where nascent peptidoglycan is modified during maturation would potentially constitute a zone of uncapped peptidoglycan. As long as cell wall synthesis is in progress, this uncapped substrate is unavailable for LytA, but when growth is inhibited by cell wall-targeting antibiotics or stationary phase entry, the cell wall synthesis machinery leaves

LytA Requires Access to the Nascent Peptidoglycan
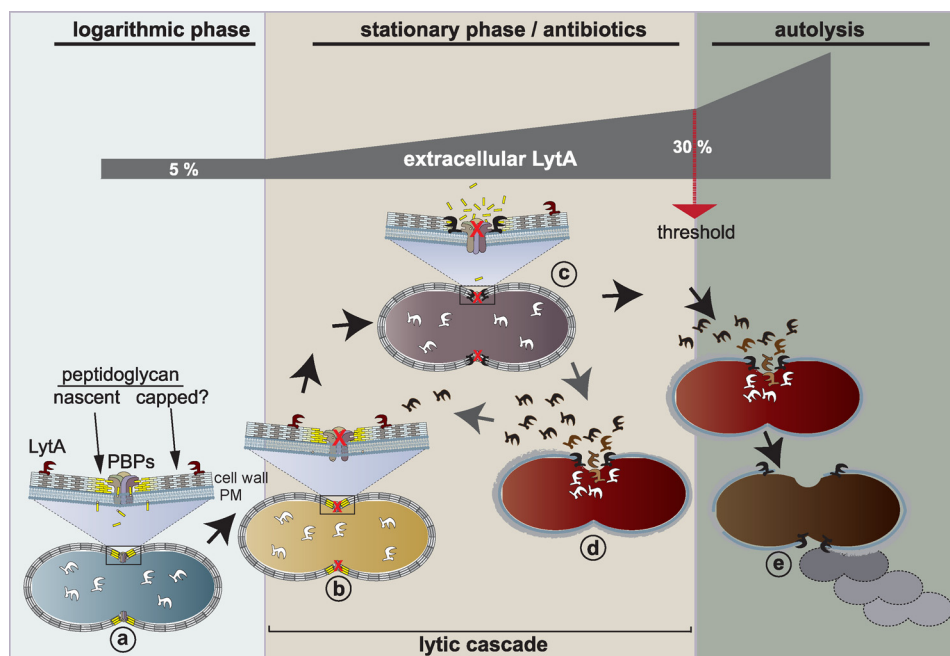
FIGURE 7. **Model for LytA activation.** *a*, a small amount (~5%) of LytA is cell wall-associated during the logarithmic phase but cannot execute any lytic activity, whereas growth and cell wall synthesis by the plasma membrane (*PM*)-associated penicillin-binding proteins (*PBPs*) is in progress. We hypothesize that the inability of LytA to induce lysis is due to capped mature peptidoglycan. *b*, upon entry into the stationary phase or through challenge with cell wall-targeting antibiotics, the cell wall synthesis machinery becomes inactive, potentially exposing the nascent and yet uncapped peptidoglycan (*c*), making it available for LytA to initiate cell wall hydrolysis. *d*, cell wall degradation leads to lysis and release of LytA from the cytoplasmic pool. The newly released LytA can bind to neighboring cells in stages *b* or *c*, and the sequential steps *b–d* constitute a lytic cascade that is initiated at the entry into the stationary phase, causing an accumulation of extracellular LytA. Autolysis is triggered when extracellular LytA reaches ~30% of total LytA (or ~0.5 μg/ml), leading to excessive lysis of most cells in the culture (*e*).

its tight association with the nascent peptidoglycan, and LytA may gain access to this uncapped peptidoglycan and initiate cell wall degradation.

A model is provided that summarizes our results and suggestions. We found that the majority of LytA resides in the cytoplasm during growth and that only a small fraction of LytA is extracellular in association with the cell wall (Fig. 7*a*). As long as growth progresses and cell wall synthesis is active, the cells are protected from LytA, and we hypothesize that this is due to capped peptidoglycan. When growth is halted due to stationary phase entry or antibiotic treatment, the cell wall synthesis machinery becomes inactive (Fig. 7*b*). On the basis of the observation that a substrate for the amidase domain of LytA is present within the nascent peptidoglycan, we suggest that LytA needs access to this region to initiate cell wall degradation (Fig. 7*c*). A possible scenario is that LytA works as an exo-amidase that needs some type of open-ended structure to initiate cell wall degradation. Continued cell wall degradation leads to lysis, which releases intracellular LytA from the cytoplasmic compartment (Fig. 7*d*). The released LytA can, in turn, bind to the cell wall of neighboring intact cells, and this process (Fig. 7, *b–d*) constitutes a lytic cascade leading to an accumulation of extracellular LytA. Autolysis is induced when a critical threshold concentration is reached corresponding to ~30% of extracellular LytA (or ~0.5 μg/ml), leading to excessive lysis of most cells in the culture (Fig. 7*e*). Further studies are warranted to identify whether pneumococci cap their cell wall, how this is achieved, and whether this mechanism applies to other Gram-positive bacteria.

REFERENCES

1. Neufeld, F. (1900) Über eine specifische bakteriolytische Wirkung der Galle. *Z. Hyg. Infektionskr.* **34,** 454–464
2. Avery, O. T., and Cullen, G. E. (1923) Studies on the Enzymes of *Pneumococcus*. IV. Bacteriolytic Enzyme. *J. Exp. Med.* **38,** 199–206
3. Goebel, W. F., and Avery, O. T. (1929) A Study of *Pneumococcus* Autolysis. *J. Exp. Med.* **49,** 267–286
4. Tomasz, A., Albino, A., and Zanati, E. (1970) Multiple antibiotic resistance in a bacterium with suppressed autolytic system. *Nature* **227,** 138–140
5. Tomasz, A., and Waks, S. (1975) Mechanism of action of penicillin. Triggering of the pneumococcal autolytic enzyme by inhibitors of cell wall synthesis. *Proc. Natl. Acad. Sci. U.S.A.* **72,** 4162–4166
6. Fernández-Tornero, C., López, R., García, E., Giménez-Gallego, G., and Romero, A. (2001) A novel solenoid fold in the cell wall anchoring domain of the pneumococcal virulence factor LytA. *Nat. Struct. Biol.* **8,** 1020–1024
7. García, E., García, J. L., Ronda, C., García, P., and López, R. (1985) Cloning and expression of the pneumococcal autolysin gene in *Escherichia coli*. *Mol. Gen. Genet.* **201,** 225–230
8. Howard, L. V., and Gooder, H. (1974) Specificity of the autolysin of *Streptococcus* (*Diplococcus*) *pneumoniae*. *J. Bacteriol.* **117,** 796–804
9. Loessner, M. J. (2005) Bacteriophage endolysins. Current state of research and applications. *Curr. Opin. Microbiol.* **8,** 480–487
10. Vollmer, W., Joris, B., Charlier, P., and Foster, S. (2008) Bacterial peptidoglycan (murein) hydrolases. *FEMS Microbiol. Rev.* **32,** 259–286
11. Mellroth, P., Karlsson, J., and Steiner, H. (2003) A scavenger function for a *Drosophila* peptidoglycan recognition protein. *J. Biol. Chem.* **278,** 7059–7064
12. Royet, J., and Dziarski, R. (2007) Peptidoglycan recognition proteins.

Pleiotropic sensors and effectors of antimicrobial defences. *Nat. Rev. Microbiol.* **5,** 264–277

13. Kang, D., Liu, G., Lundström, A., Gelius, E., and Steiner, H. (1998) A peptidoglycan recognition protein in innate immunity conserved from insects to humans. *Proc. Natl. Acad. Sci. U.S.A.* **95,** 10078–10082

14. Giudicelli, S., and Tomasz, A. (1984) Attachment of pneumococcal autolysin to wall teichoic acids, an essential step in enzymatic wall degradation. *J. Bacteriol.* **158,** 1188–1190

15. Hirst, R. A., Gosai, B., Rutman, A., Guerin, C. J., Nicotera, P., Andrew, P. W., and O'Callaghan, C. (2008) *Streptococcus pneumoniae* deficient in pneumolysin or autolysin has reduced virulence in meningitis. *J. Infect. Dis.* **197,** 744–751

16. Berry, A. M., and Paton, J. C. (2000) Additive attenuation of virulence of *Streptococcus pneumoniae* by mutation of the genes encoding pneumolysin and other putative pneumococcal virulence proteins. *Infect. Immun.* **68,** 133–140

17. Canvin, J. R., Marvin, A. P., Sivakumaran, M., Paton, J. C., Boulnois, G. J., Andrew, P. W., and Mitchell, T. J. (1995) The role of pneumolysin and autolysin in the pathology of pneumonia and septicemia in mice infected with a type 2 pneumococcus. *J. Infect. Dis.* **172,** 119–123

18. Martner, A., Dahlgren, C., Paton, J. C., and Wold, A. E. (2008) Pneumolysin released during *Streptococcus pneumoniae* autolysis is a potent activator of intracellular oxygen radical production in neutrophils. *Infect. Immun.* **76,** 4079–4087

19. Eldholm, V., Johnsborg, O., Haugen, K., Ohnstad, H. S., and Håvarstein, L. S. (2009) Fratricide in *Streptococcus pneumoniae.* Contributions and role of the cell wall hydrolases CbpD, LytA and LytC. *Microbiology* **155,** 2223–2234

20. Martner, A., Skovbjerg, S., Paton, J. C., and Wold, A. E. (2009) *Streptococcus pneumoniae* autolysis prevents phagocytosis and production of phagocyte-activating cytokines. *Infect. Immun.* **77,** 3826–3837

21. Moreillon, P., and Tomasz, A. (1988) Penicillin resistance and defective lysis in clinical isolates of pneumococci. Evidence for two kinds of antibiotic pressure operating in the clinical environment. *J. Infect. Dis.* **157,** 1150–1157

22. Moscoso, M., Domenech, M., and Garcia, E. (2010) Vancomycin tolerance in clinical and laboratory *Streptococcus pneumoniae* isolates depends on reduced enzyme activity of the major LytA autolysin or cooperation between CiaH histidine kinase and capsular polysaccharide. *Mol. Microbiol.* **77,** 1052–1064

23. Lacks, S., and Hotchkiss, R. D. (1960) A study of the genetic material determining an enzyme in *Pneumococcus. Biochim. Biophys. Acta* **39,** 508–518

24. Daniels, R., Mellroth, P., Bernsel, A., Neiers, F., Normark, S., von Heijne, G., and Henriques-Normark, B. (2010) Disulfide bond formation and cysteine exclusion in gram-positive bacteria. *J. Biol. Chem.* **285,** 3300–3309

25. Neumann, D., Bückers, J., Kastrup, L., Hell, S. W., and Jakobs, S. (2010) Two-color STED microscopy reveals different degrees of colocalization between hexokinase-I and the three human VDAC isoforms. *PMC Biophys.* **3,** 4

26. Wildanger, D., Rittweger, E., Kastrup, L., and Hell, S. W. (2008) STED microscopy with a supercontinuum laser source. *Opt. Express.* **16,** 9614–9621

27. Sanchez-Puelles, J. M., Ronda, C., Garcia, J. L., Garcia, P., Lopez, R., and Garcia, E. (1986) Searching for autolysin functions. Characterization of a pneumococcal mutant deleted in the lytA gene. *Eur. J. Biochem.* **158,** 289–293

28. Hakenbeck, R., Madhour, A., Denapaite, D., and Brückner, R. (2009) Versatility of choline metabolism and choline-binding proteins in *Streptococcus pneumoniae* and commensal streptococci. *FEMS Microbiol. Rev.* **33,** 572–586

29. Frolet, C., Beniazza, M., Roux, L., Gallet, B., Noirclerc-Savoye, M., Vernet, T., and Di Guilmi, A. M. (2010) New adhesin functions of surface-exposed pneumococcal proteins. *BMC Microbiol.* **10,** 190

30. Claverys, J. P., Martin, B., and Håvarstein, L. S. (2007) Competence-induced fratricide in streptococci. *Mol. Microbiol.* **64,** 1423–1433

31. Håvarstein, L. S., Martin, B., Johnsborg, O., Granadel, C., and Claverys, J. P. (2006) New insights into the pneumococcal fratricide. Relationship to clumping and identification of a novel immunity factor. *Mol. Microbiol.* **59,** 1297–1307

32. Carlsson, F., Stålhammar-Carlemalm, M., Flärdh, K., Sandin, C., Carlemalm, E., and Lindahl, G. (2006) Signal sequence directs localized secretion of bacterial surface proteins. *Nature* **442,** 943–946

33. DeDent, A., Bae, T., Missiakas, D. M., and Schneewind, O. (2008) Signal peptides direct surface proteins to two distinct envelope locations of *Staphylococcus aureus. EMBO J.* **27,** 2656–2668

34. Zoll, S., Pätzold, B., Schlag, M., Götz, F., Kalbacher, H., and Stehle, T. (2010) Structural basis of cell wall cleavage by a staphylococcal autolysin. *PLoS Pathog.* **6,** e1000807

35. Zapun, A., Vernet, T., and Pinho, M. G. (2008) The different shapes of cocci. *FEMS Microbiol. Rev.* **32,** 345–360

36. Crisóstomo, M. I., Vollmer, W., Kharat, A. S., Inhülsen, S., Gehre, F., Buckenmaier, S., and Tomasz, A. (2006) Attenuation of penicillin resistance in a peptidoglycan *O*-acetyl transferase mutant of *Streptococcus pneumoniae. Mol. Microbiol.* **61,** 1497–1509

37. Vollmer, W., and Tomasz, A. (2000) The pgdA gene encodes for a peptidoglycan N-acetylglucosamine deacetylase in *Streptococcus pneumoniae. J. Biol. Chem.* **275,** 20496–20501

38. Filipe, S. R., and Tomasz, A. (2000) Inhibition of the expression of penicillin resistance in *Streptococcus pneumoniae* by inactivation of cell wall muropeptide branching genes. *Proc. Natl. Acad. Sci. U.S.A.* **97,** 4891–4896